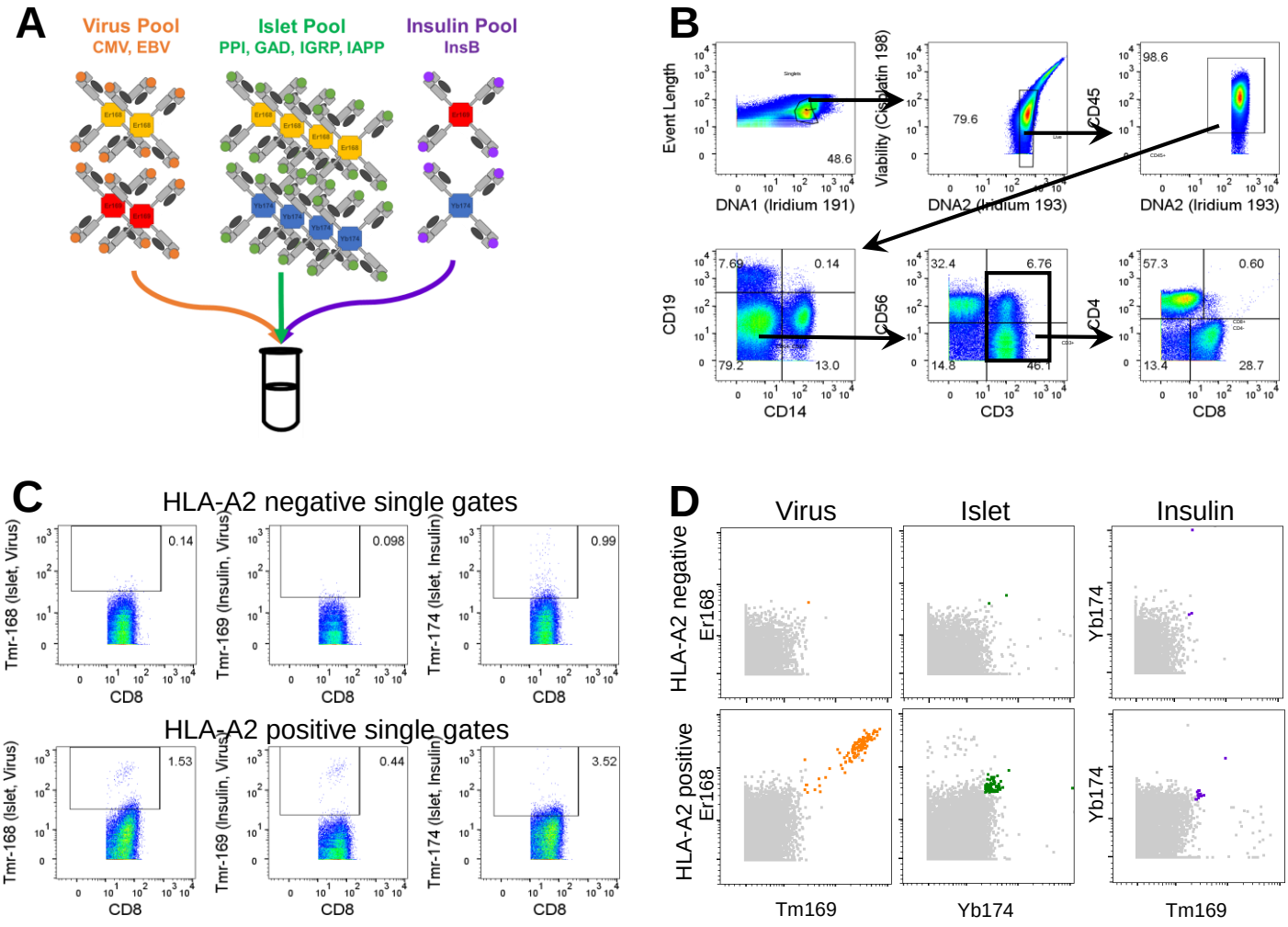

Supplemental Figure 1. Detection of antigen-specific CD8⁺ T cell populations using combinatorial Tmr staining. **(A)** Schematic of the semi-combinatorial pooled antigen Tmr staining. **(B)** Total events were manually gated on singlet live cells that were $CD45^{+}CD14^{-}CD19^{-}CD3^{+}CD4^{-}CD8^{+}$ to identify $CD8^{+}$ T cells. **(C)** Each of the three Tmr labels for HLA-A2 negative controls and positive samples were gated within total $CD8^{+}$ T cells. **(D)** Boolean gating was applied to identify cells that were labelled with two of the three metal isotopes, but not the third. Tmr^{+} limit of detection was 0.02% of total $CD8^{+}$ T cells determined by a spike-in clone and all samples included >10,000 total $CD8^{+}$ T cells. Representative examples from an HLA-A2 negative or positive individual in which virus- (orange), islet- (green), or insulin-specific (purple) $CD8^{+}$ T cells were identified and overlaid on total CD8 T cells (gray). Tmr, tetramer.

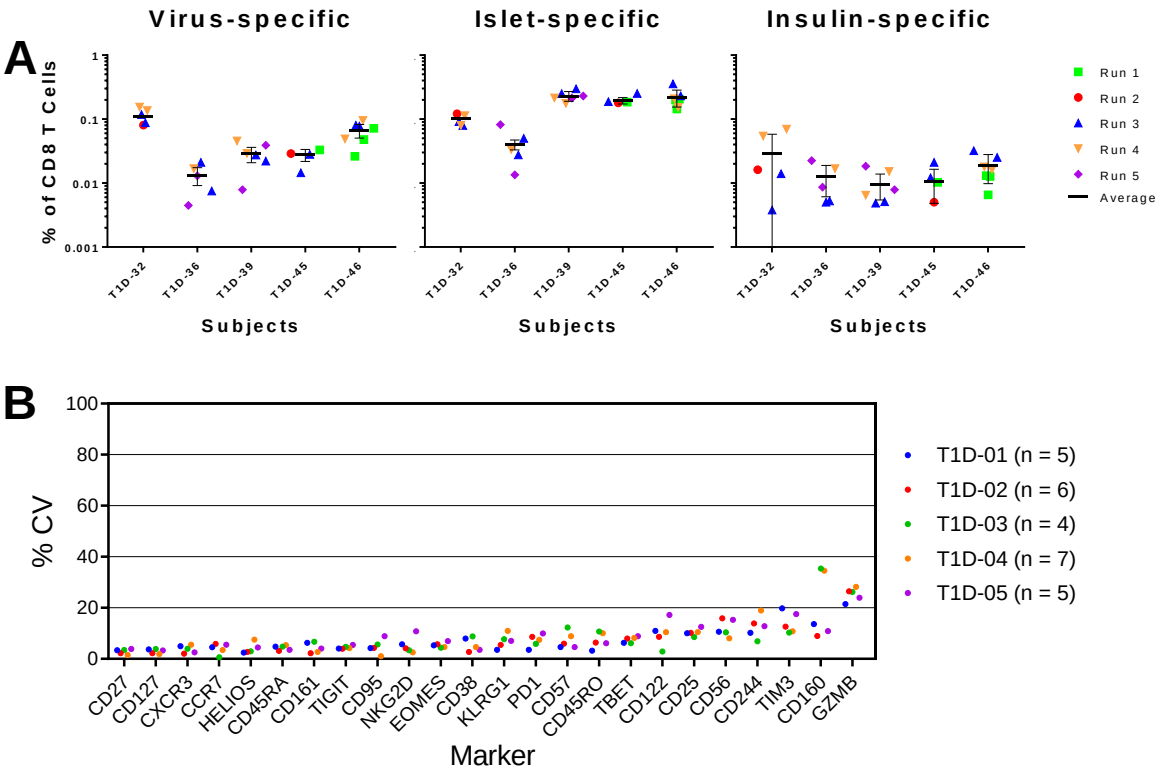

Supplemental Figure 2. Reproducible detection and phenotyping of antigen-specific CD8⁺ T cell populations. Five T1D subjects (Supplemental Table 3) with multiple aliquots of cryopreserved PBMC were thawed, stained, and acquired using a 35-parameter mass cytometry panel on three separate days (runs) per subject, with replicates performed on selected days. Total and antigen-specific CD8⁺ T cells were gated as in Supplemental Figure 1. **(A)** Frequency of antigen-specific CD8⁺ T cells; mean % coefficient of variation (CV) for virus-, islet-, and insulin-specific CD8⁺ T cells of 27 ± 4%, 19 ± 7%, and 59 ± 23, respectively. Black horizontal lines with error bars represent geometric mean ± geometric SD. **(B)** %CV of the mean hyperbolic arcsine-transformed intensity of each of 24 markers on CD8⁺ T cells across all replicates for each of the five subjects. CV, coefficient of variation.

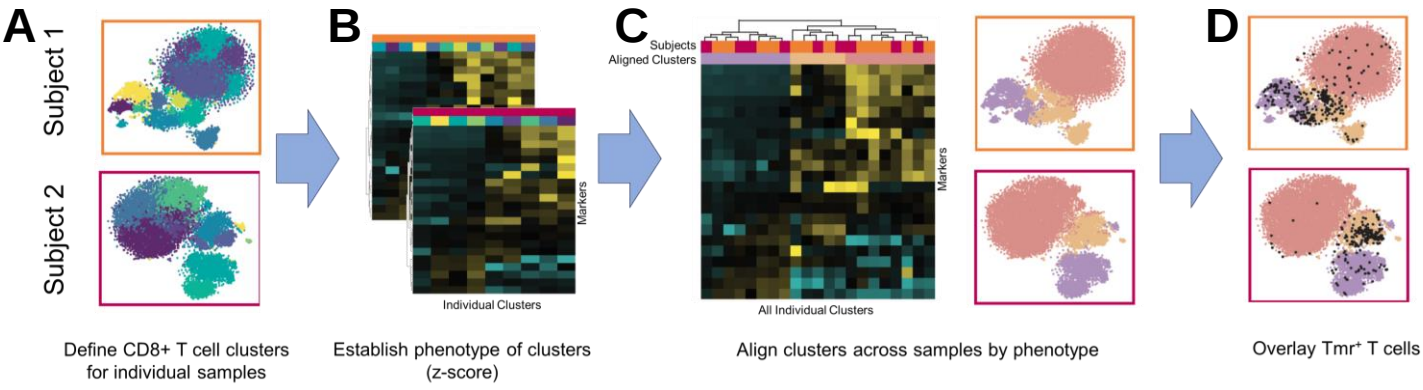

Supplemental Figure 3. Details of DISCOV-R (DIStribution analysis across Clusters of a parent population OVerlaid with a Rare subpopulation). DISCOV-R was applied to two representative subjects (orange or pink) that were assayed with a 35-parameter CyTOF panel to identify and phenotype antigen-specific (Tmr^+) $CD8^+$ T cells. **(A)** The parent population ($CD8^+$ T cells) is clustered for each individual using Phenograph and visualized on a 2D tSNE (clusters represented as colors). **(B)** Z-score normalized average expression (compared to total $CD8^+$ T cells) of all phenotyping markers for all clusters from individual samples. **(C)** Hierarchical clustering of average z-score normalized expression of all clusters from all individual samples to align clusters across samples (three, indicated by color in bar at top of graph). **(D)** Islet-specific (Tmr^+) $CD8^+$ T cell events are overlaid onto the aligned clusters to assess their distribution. Tmr, tetramer.

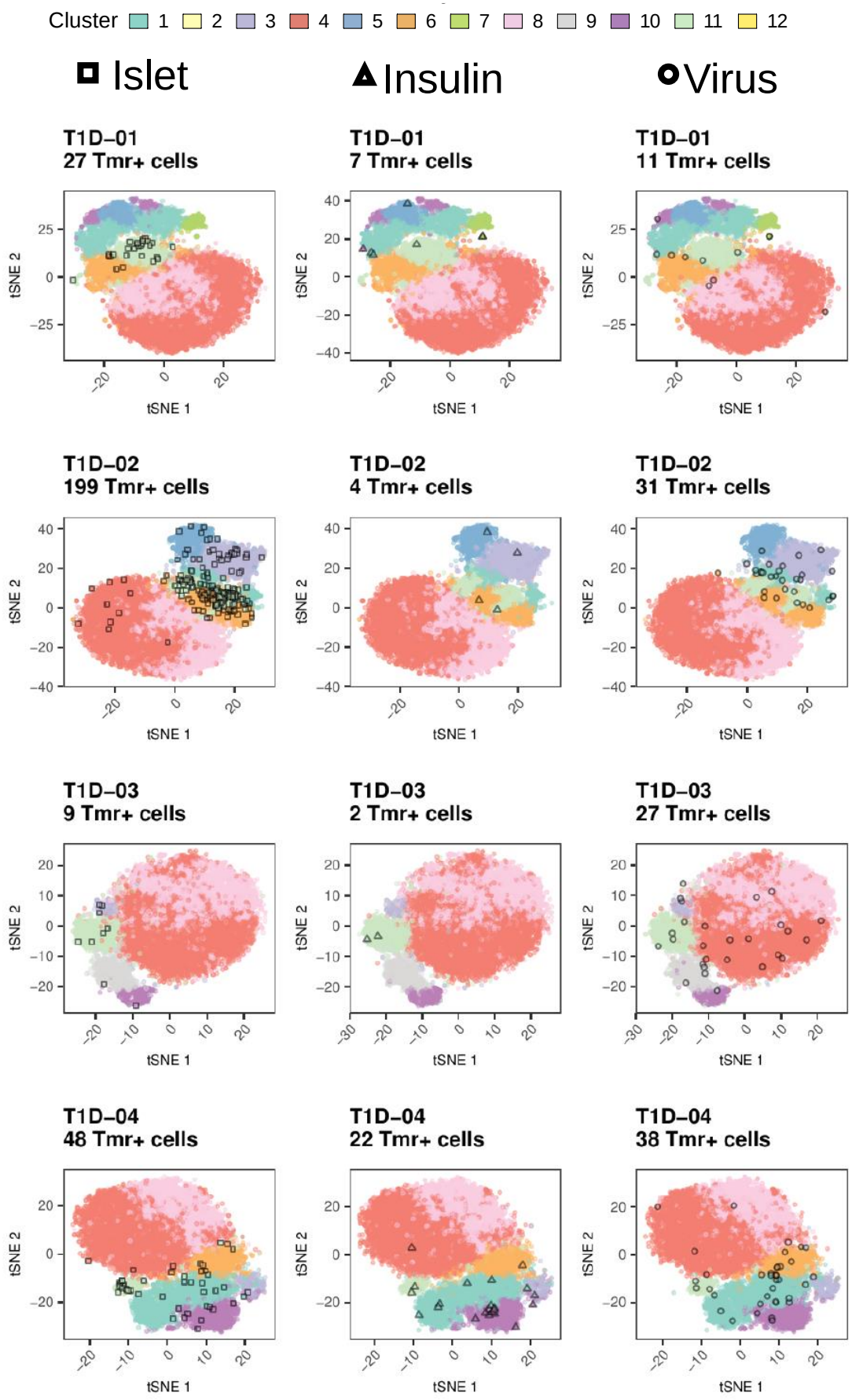
Cluster 1 2 3 4 5 6 7 8 9 10 11 12
Islet
Insulin
Virus
T1D–01
27 Tmr+ cells
T1D–01
7 Tmr+ cells
T1D–01
11 Tmr+ cells
T1D–02
199 Tmr+ cells
T1D–02
4 Tmr+ cells
T1D–02
31 Tmr+ cells
T1D–03
9 Tmr+ cells
T1D–03
2 Tmr+ cells
T1D–03
27 Tmr+ cells
T1D–04
48 Tmr+ cells
T1D–04
22 Tmr+ cells
T1D–04
38 Tmr+ cells
tSNE 1
tSNE 2

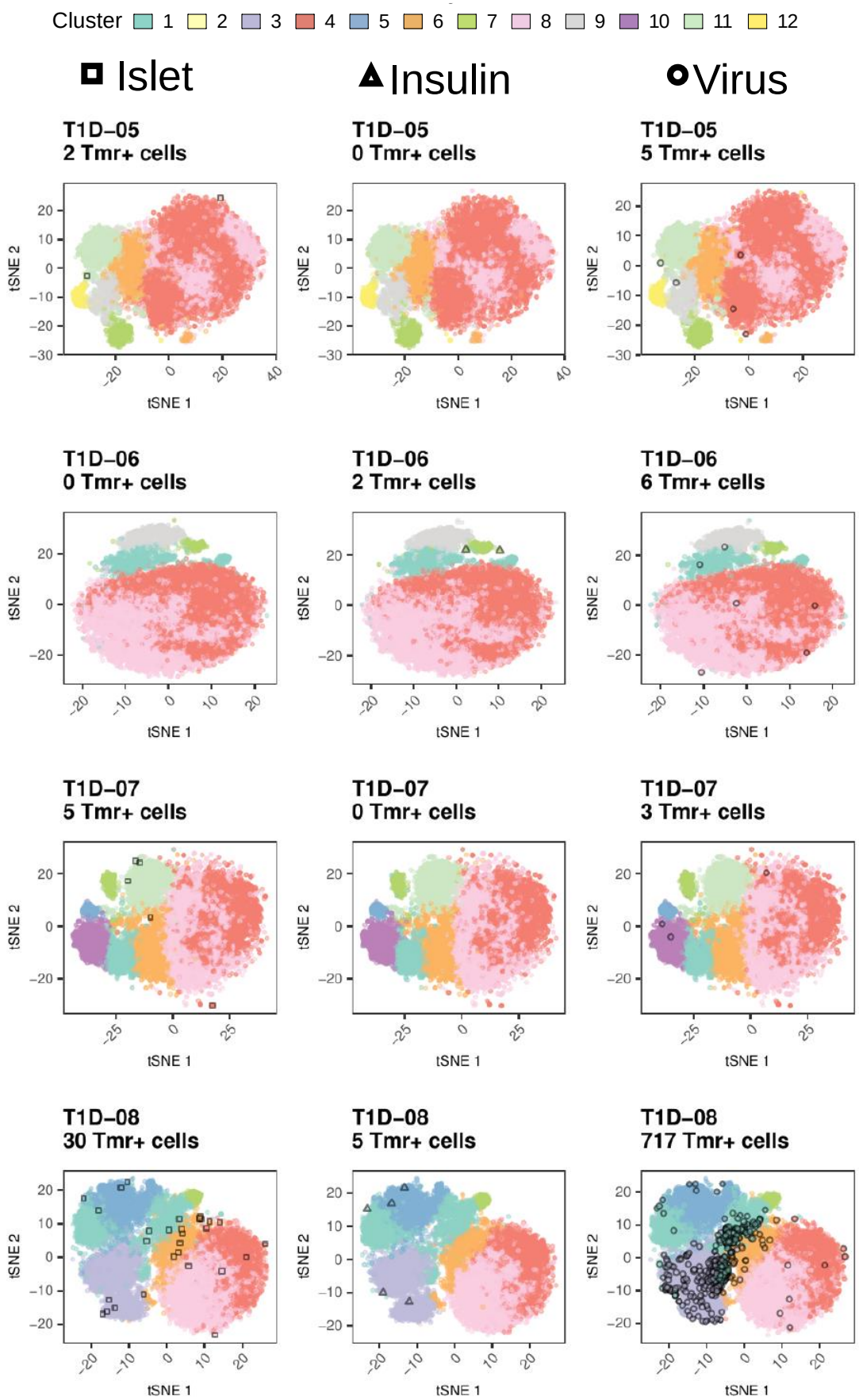
Cluster 1 2 3 4 5 6 7 8 9 10 11 12
Islet
Insulin
Virus
T1D–05
2 Tmr+ cells
T1D–05
0 Tmr+ cells
T1D–05
5 Tmr+ cells
T1D–06
0 Tmr+ cells
T1D–06
2 Tmr+ cells
T1D–06
6 Tmr+ cells
T1D–07
5 Tmr+ cells
T1D–07
0 Tmr+ cells
T1D–07
3 Tmr+ cells
T1D–08
30 Tmr+ cells
T1D–08
5 Tmr+ cells
T1D–08
717 Tmr+ cells
tSNE 1
tSNE 2

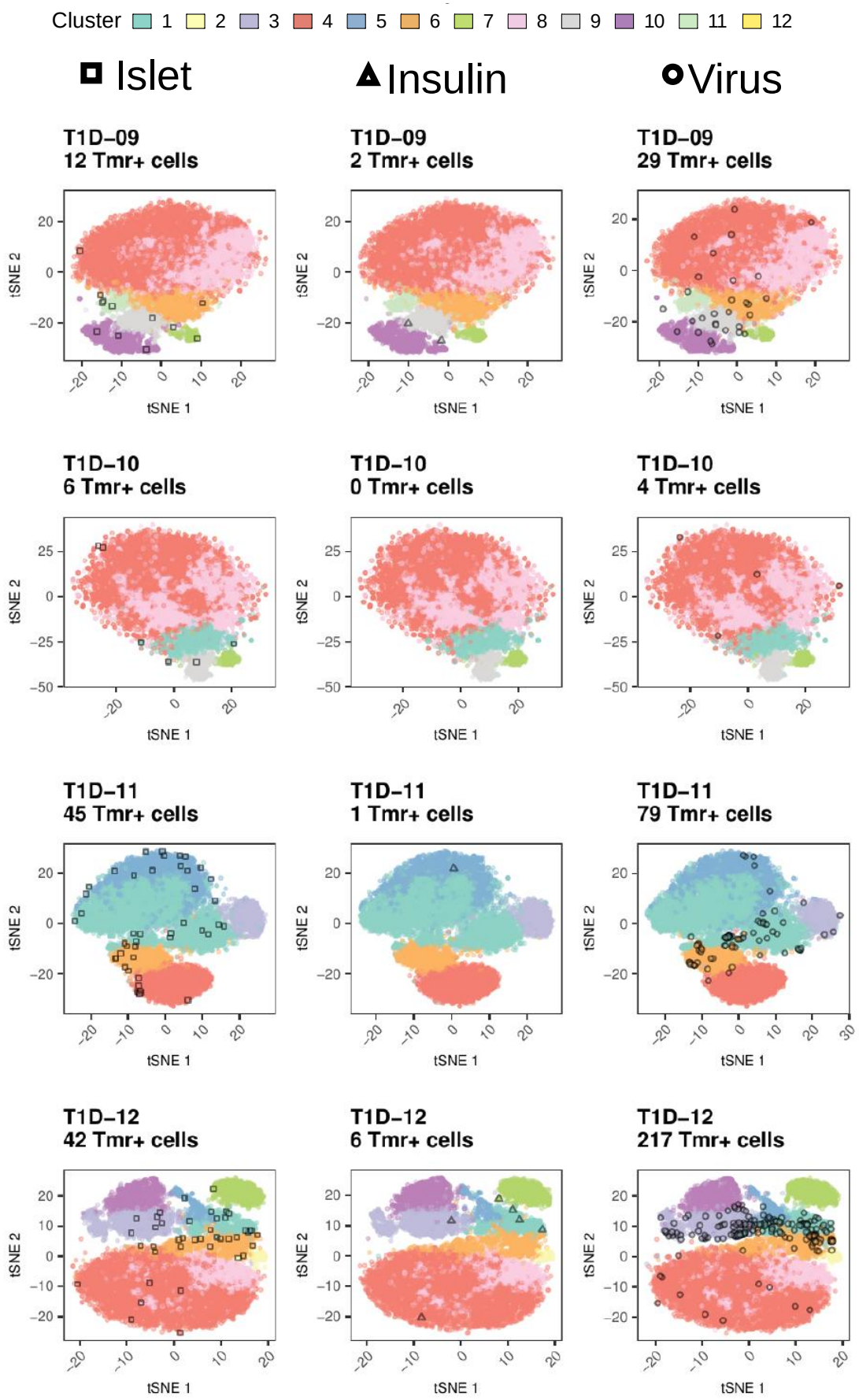
Cluster 1 2 3 4 5 6 7 8 9 10 11 12
Islet
Insulin
Virus
T1D–09
12 Tmr+ cells
T1D–09
2 Tmr+ cells
T1D–09
29 Tmr+ cells
T1D–10
6 Tmr+ cells
T1D–10
0 Tmr+ cells
T1D–10
4 Tmr+ cells
T1D–11
45 Tmr+ cells
T1D–11
1 Tmr+ cells
T1D–11
79 Tmr+ cells
T1D–12
42 Tmr+ cells
T1D–12
6 Tmr+ cells
T1D–12
217 Tmr+ cells
tSNE 1
tSNE 2

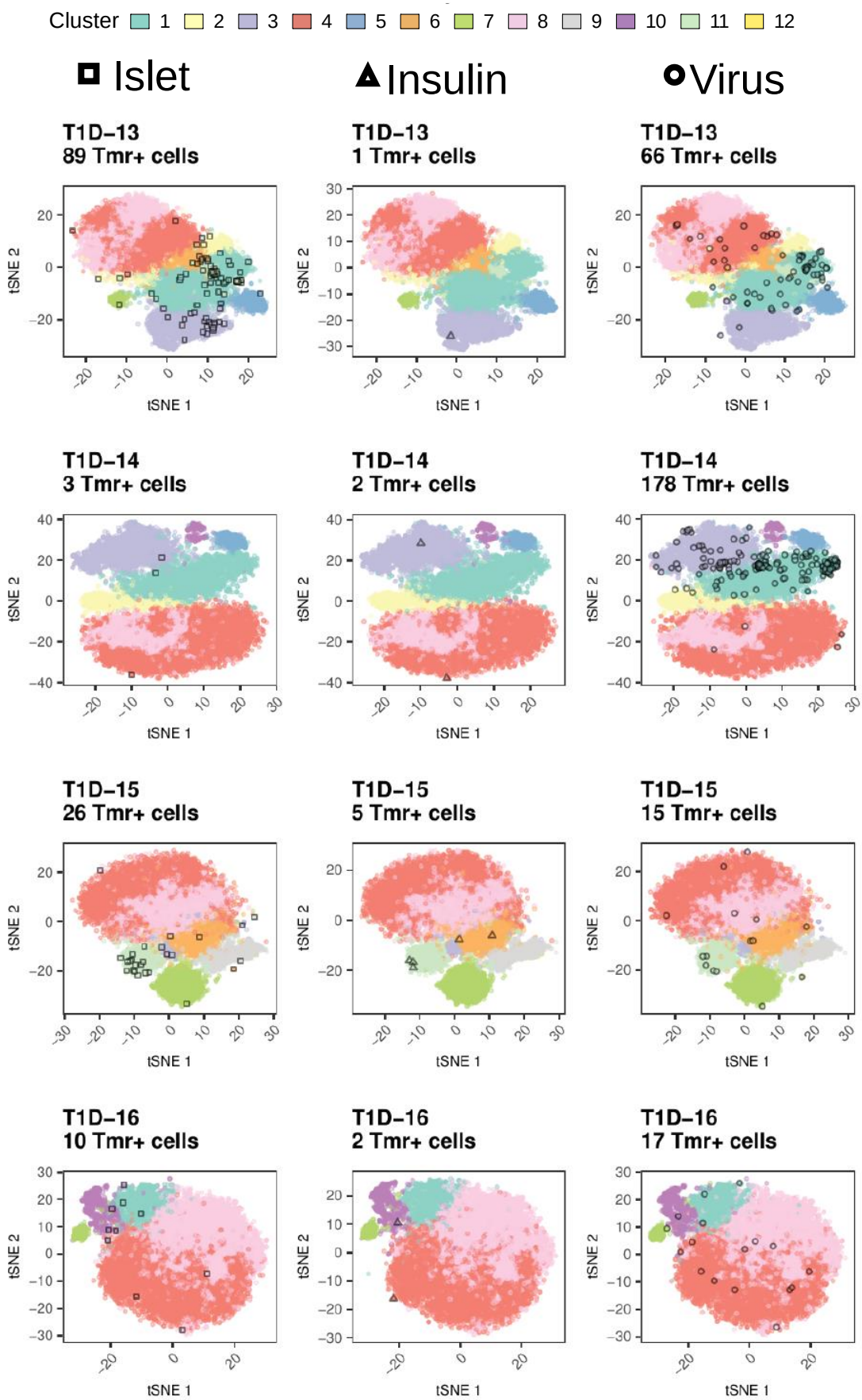
Cluster 1 2 3 4 5 6 7 8 9 10 11 12
Islet
Insulin
Virus
T1D–13
89 Tmr+ cells
T1D–13
1 Tmr+ cells
T1D–13
66 Tmr+ cells
T1D–14
3 Tmr+ cells
T1D–14
2 Tmr+ cells
T1D–14
178 Tmr+ cells
T1D–15
26 Tmr+ cells
T1D–15
5 Tmr+ cells
T1D–15
15 Tmr+ cells
T1D–16
10 Tmr+ cells
T1D–16
2 Tmr+ cells
T1D–16
17 Tmr+ cells
tSNE 1
tSNE 2

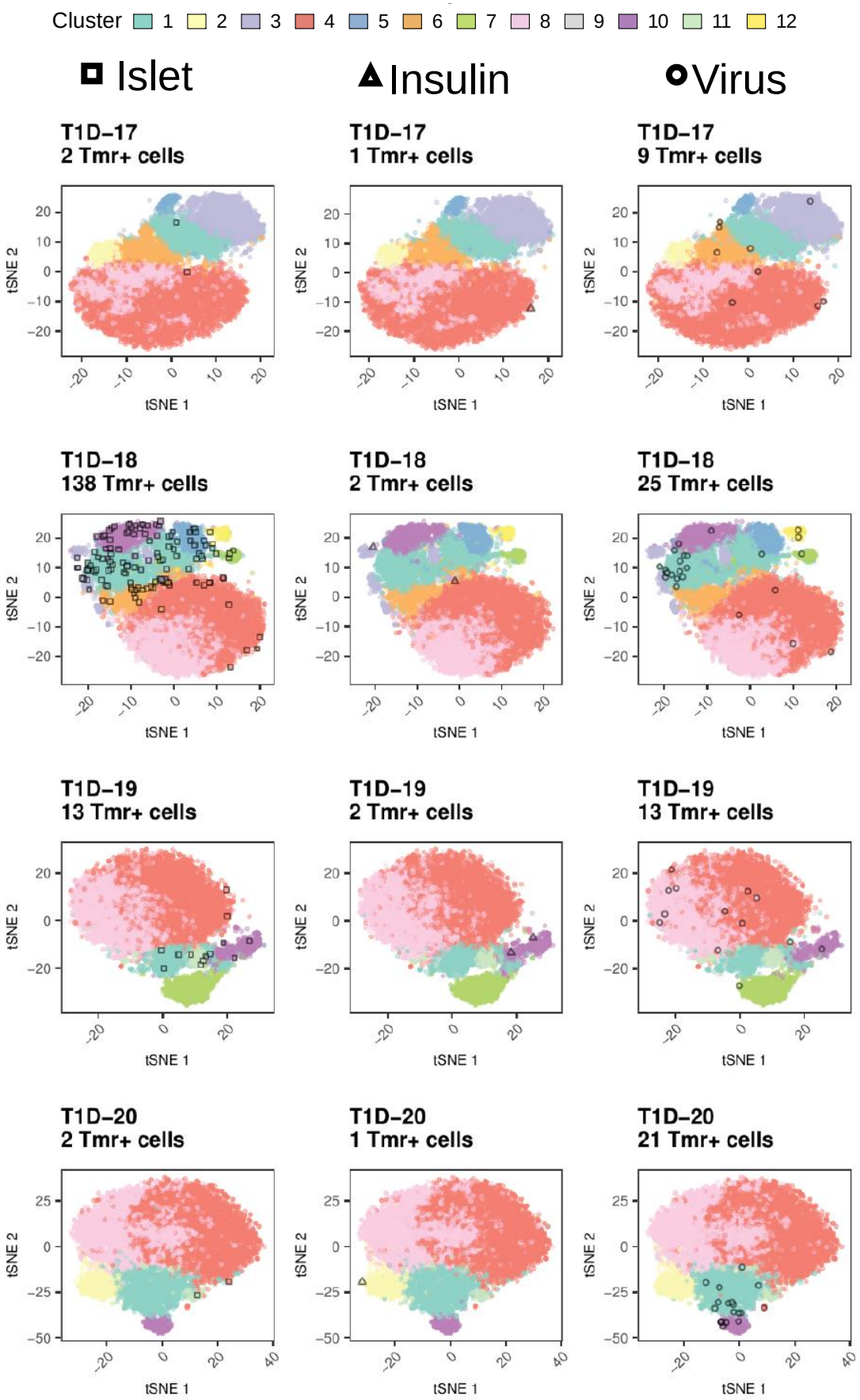
Cluster 1 2 3 4 5 6 7 8 9 10 11 12
Islet
Insulin
Virus
T1D–17
2 Tmr+ cells
T1D–17
1 Tmr+ cells
T1D–17
9 Tmr+ cells
T1D–18
138 Tmr+ cells
T1D–18
2 Tmr+ cells
T1D–18
25 Tmr+ cells
T1D–19
13 Tmr+ cells
T1D–19
2 Tmr+ cells
T1D–19
13 Tmr+ cells
T1D–20
2 Tmr+ cells
T1D–20
1 Tmr+ cells
T1D–20
21 Tmr+ cells
tSNE 1
tSNE 2

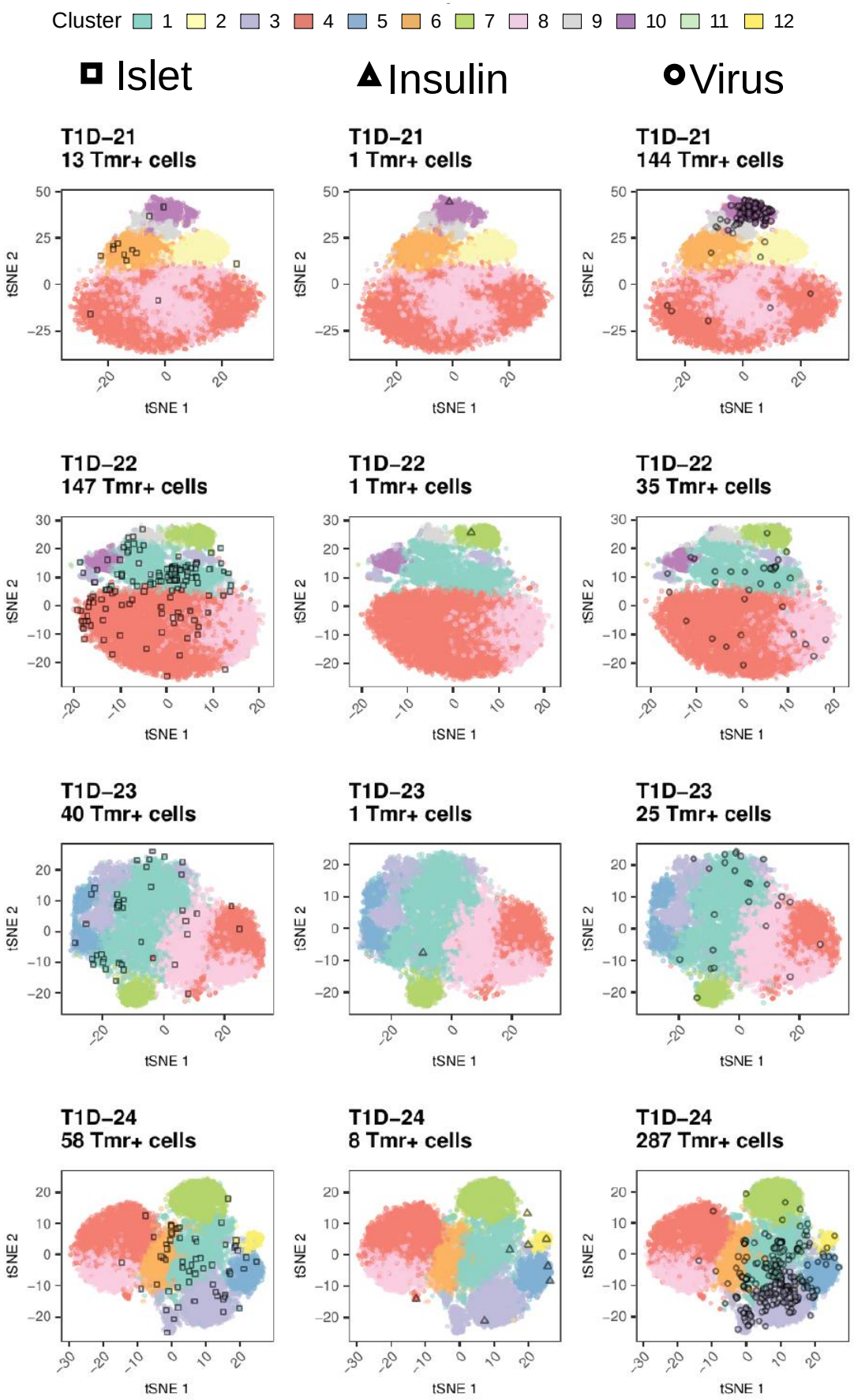
Cluster 1 2 3 4 5 6 7 8 9 10 11 12
Islet
Insulin
Virus
T1D–21
13 Tmr+ cells
T1D–21
1 Tmr+ cells
T1D–21
144 Tmr+ cells
T1D–22
147 Tmr+ cells
T1D–22
1 Tmr+ cells
T1D–22
35 Tmr+ cells
T1D–23
40 Tmr+ cells
T1D–23
1 Tmr+ cells
T1D–23
25 Tmr+ cells
T1D–24
58 Tmr+ cells
T1D–24
8 Tmr+ cells
T1D–24
287 Tmr+ cells
tSNE 1
tSNE 2

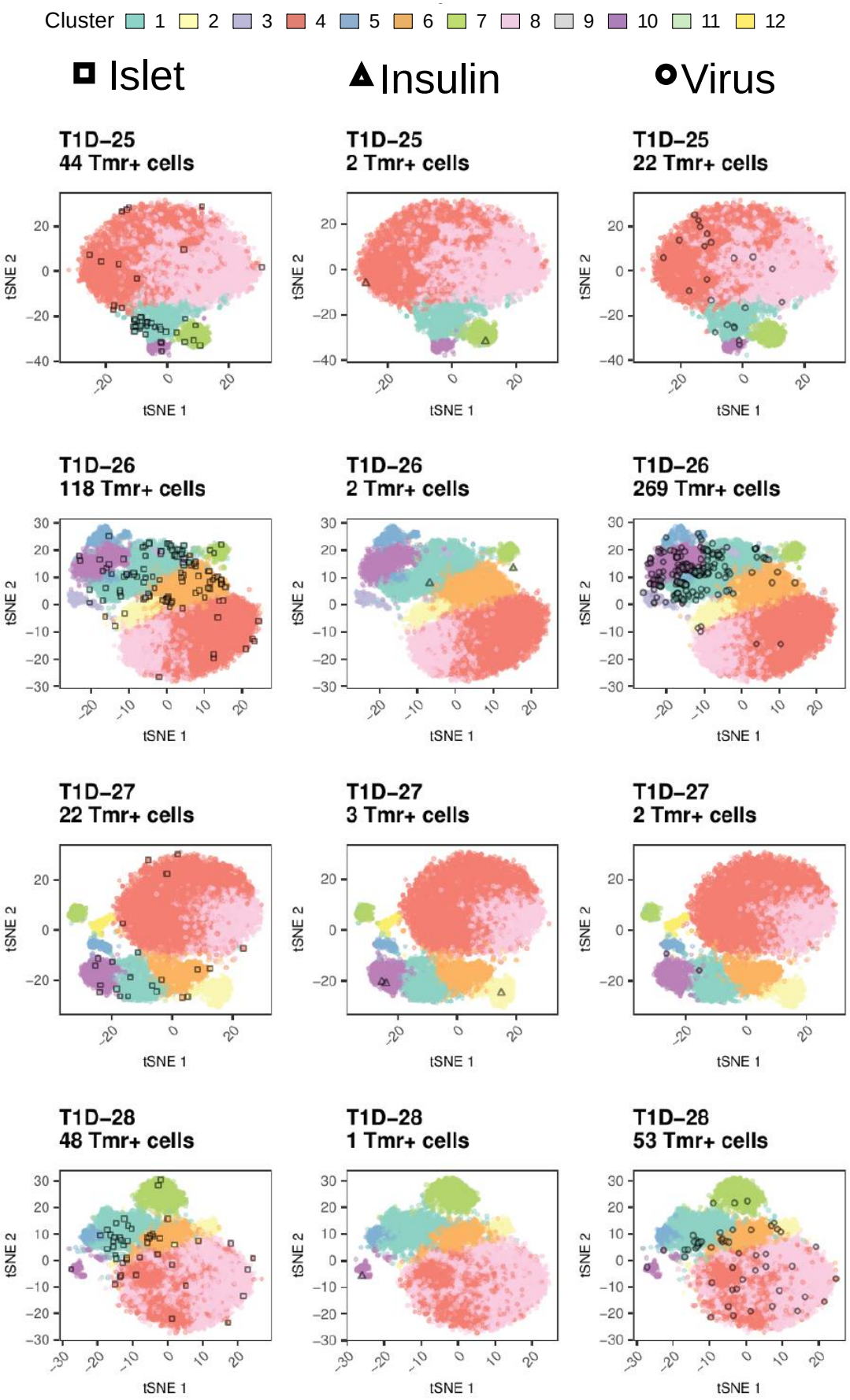
Cluster 1 2 3 4 5 6 7 8 9 10 11 12
Islet
Insulin
Virus
T1D–25
44 Tmr+ cells
T1D–25
2 Tmr+ cells
T1D–25
22 Tmr+ cells
T1D–26
118 Tmr+ cells
T1D–26
2 Tmr+ cells
T1D–26
269 Tmr+ cells
T1D–27
22 Tmr+ cells
T1D–27
3 Tmr+ cells
T1D–27
2 Tmr+ cells
T1D–28
48 Tmr+ cells
T1D–28
1 Tmr+ cells
T1D–28
53 Tmr+ cells
tSNE 1
tSNE 2

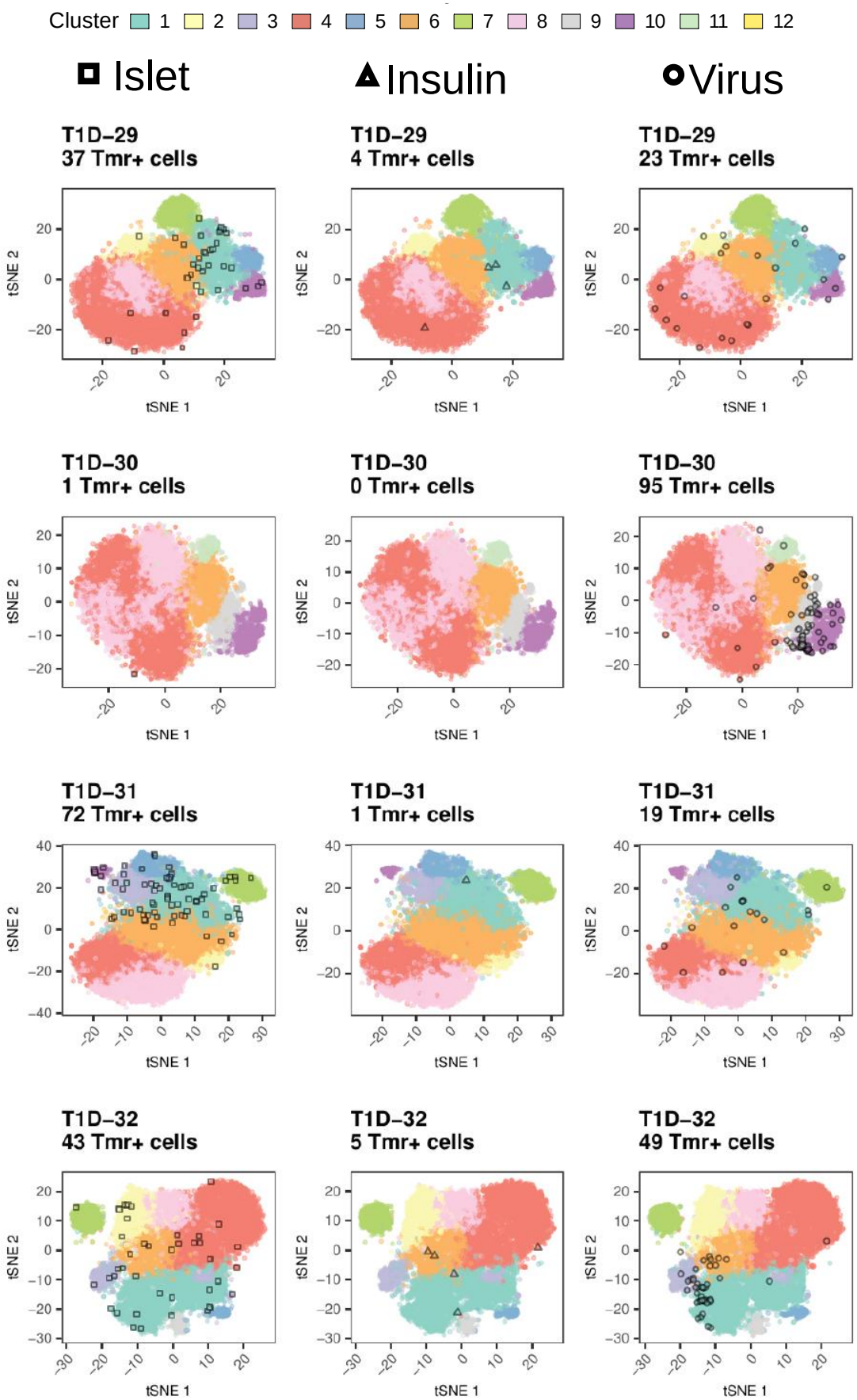
Cluster 1 2 3 4 5 6 7 8 9 10 11 12
Islet
Insulin
Virus
T1D–29
37 Tmr+ cells
T1D–29
4 Tmr+ cells
T1D–29
23 Tmr+ cells
T1D–30
1 Tmr+ cells
T1D–30
0 Tmr+ cells
T1D–30
95 Tmr+ cells
T1D–31
72 Tmr+ cells
T1D–31
1 Tmr+ cells
T1D–31
19 Tmr+ cells
T1D–32
43 Tmr+ cells
T1D–32
5 Tmr+ cells
T1D–32
49 Tmr+ cells
tSNE 1
tSNE 2

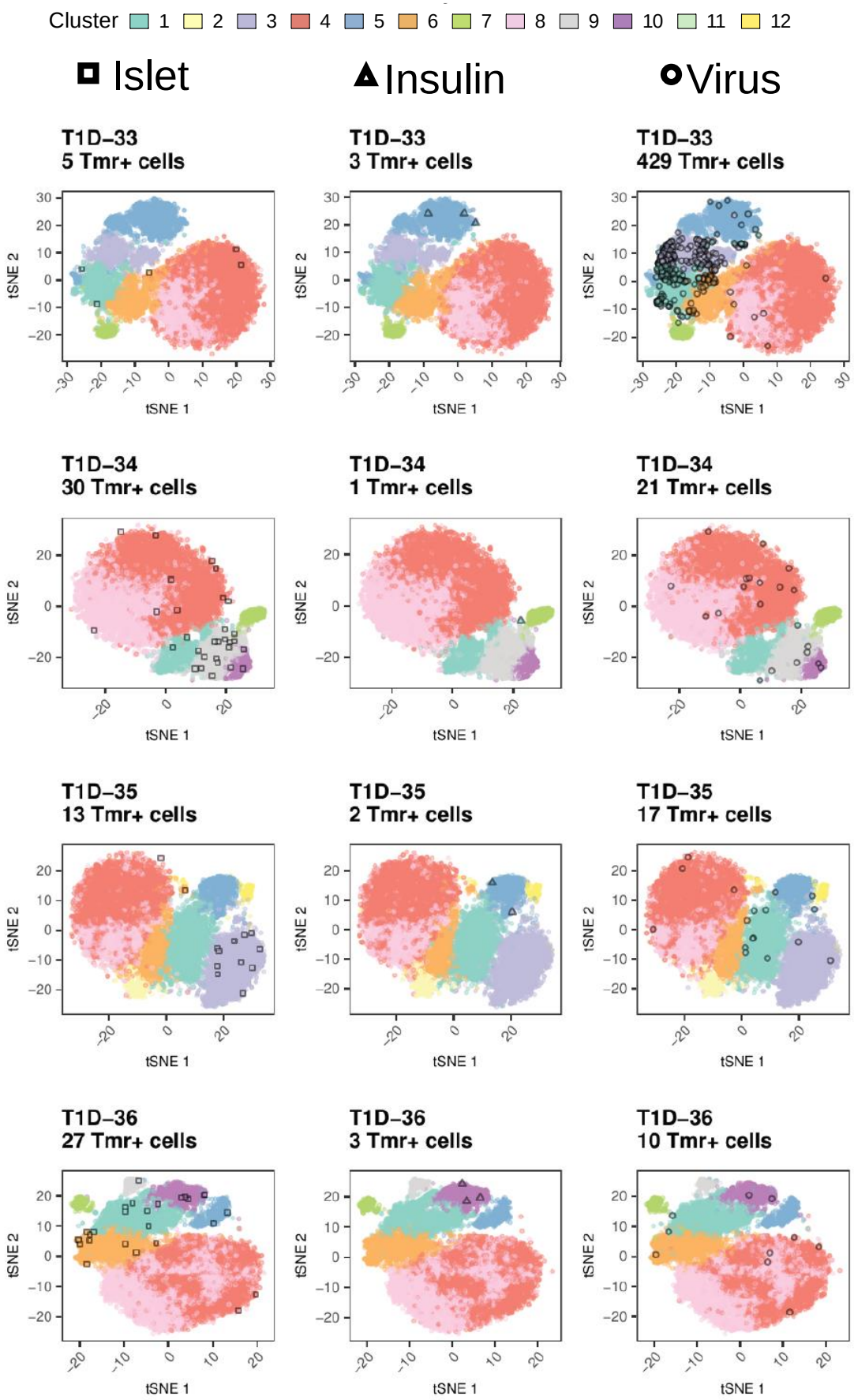
Cluster 1 2 3 4 5 6 7 8 9 10 11 12
Islet
Insulin
Virus
T1D–33
5 Tmr+ cells
T1D–33
3 Tmr+ cells
T1D–33
429 Tmr+ cells
T1D–34
30 Tmr+ cells
T1D–34
1 Tmr+ cells
T1D–34
21 Tmr+ cells
T1D–35
13 Tmr+ cells
T1D–35
2 Tmr+ cells
T1D–35
17 Tmr+ cells
T1D–36
27 Tmr+ cells
T1D–36
3 Tmr+ cells
T1D–36
10 Tmr+ cells
tSNE 1
tSNE 2

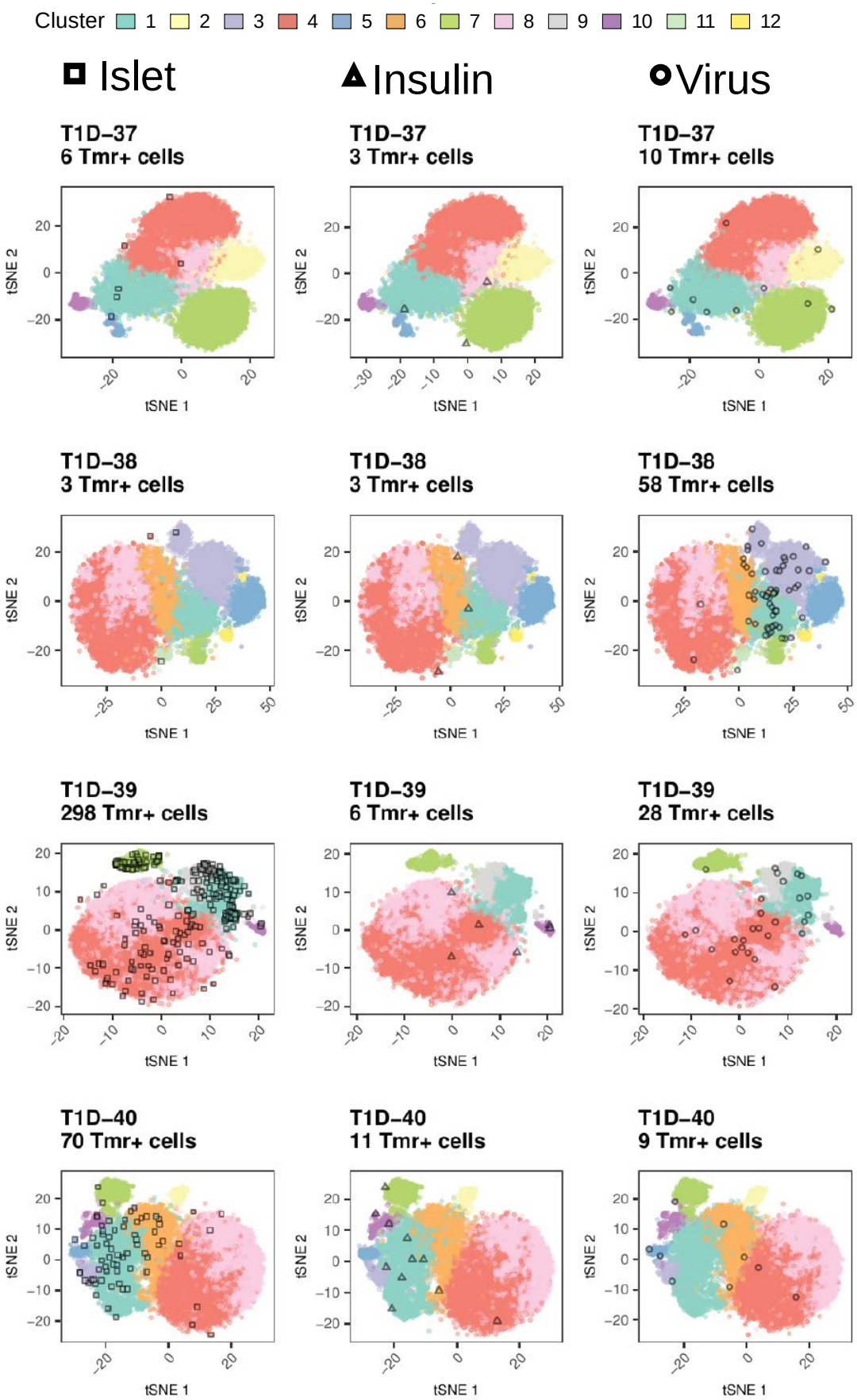
Cluster 1 2 3 4 5 6 7 8 9 10 11 12
Islet
Insulin
Virus
T1D–37
6 Tmr+ cells
T1D–37
3 Tmr+ cells
T1D–37
10 Tmr+ cells
T1D–38
3 Tmr+ cells
T1D–38
3 Tmr+ cells
T1D–38
58 Tmr+ cells
T1D–39
298 Tmr+ cells
T1D–39
6 Tmr+ cells
T1D–39
28 Tmr+ cells
T1D–40
70 Tmr+ cells
T1D–40
11 Tmr+ cells
T1D–40
9 Tmr+ cells
tSNE 1
tSNE 2

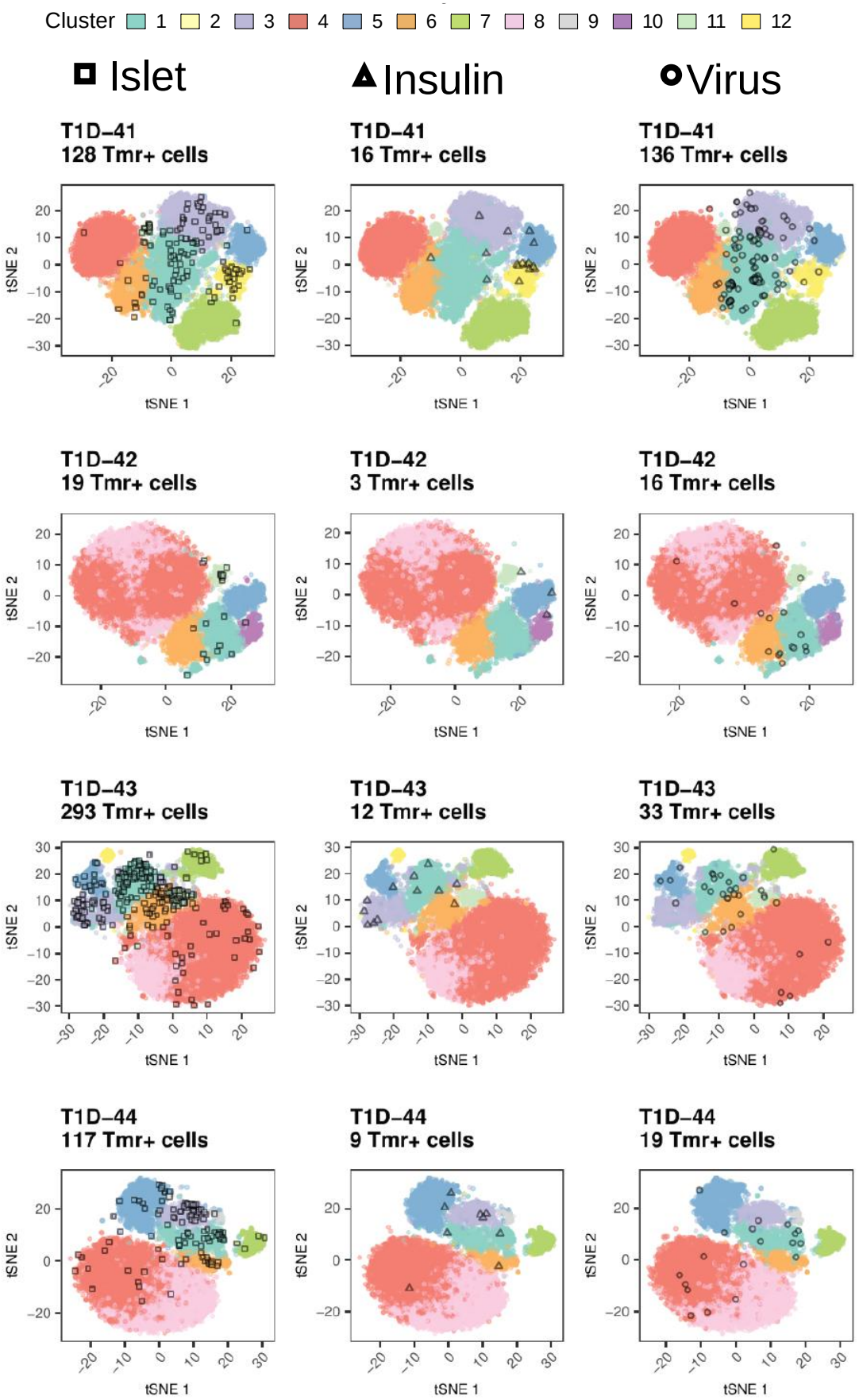
Cluster 1 2 3 4 5 6 7 8 9 10 11 12
Islet
Insulin
Virus
T1D–41
128 Tmr+ cells
T1D–41
16 Tmr+ cells
T1D–41
136 Tmr+ cells
T1D–42
19 Tmr+ cells
T1D–42
3 Tmr+ cells
T1D–42
16 Tmr+ cells
T1D–43
293 Tmr+ cells
T1D–43
12 Tmr+ cells
T1D–43
33 Tmr+ cells
T1D–44
117 Tmr+ cells
T1D–44
9 Tmr+ cells
T1D–44
19 Tmr+ cells
tSNE 1
tSNE 2

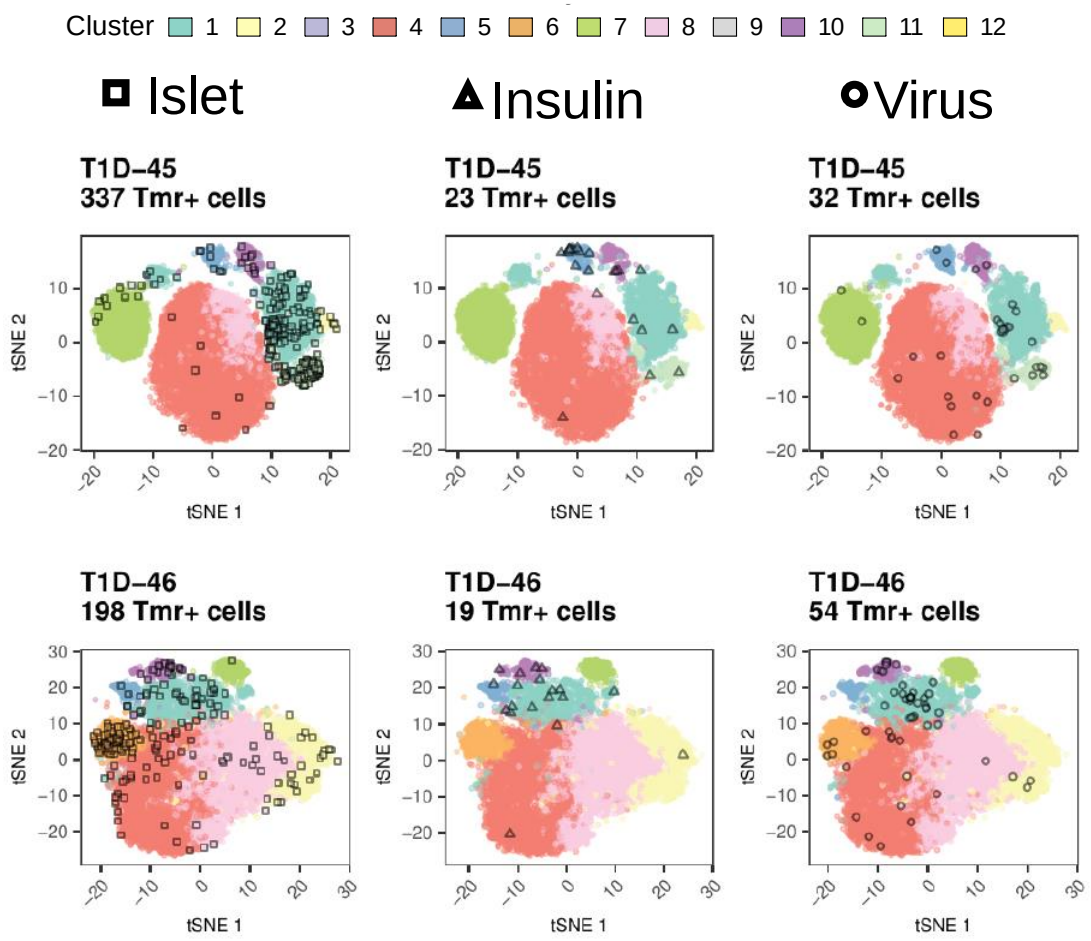

Supplemental Figure 4. Distribution of antigen-specific CD8⁺ T cells across aligned clusters for individual T1D samples. The DISCOV-R analysis method was applied to total CD8⁺ and antigen-specific T cells from T1D subjects (n=46) that were assayed with our Tmr-CyTOF panel. Shown are overlays of antigen-specific CD8⁺ T cells (squares, islet-specific; triangles, insulin-specific; circles, virus-specific) on the CD8⁺ T cell landscape for each subject, colored by aligned cluster. Clusters 1, 11, and 12 were dominant among islet-specific cells. Tmr⁺, tetramer positive.

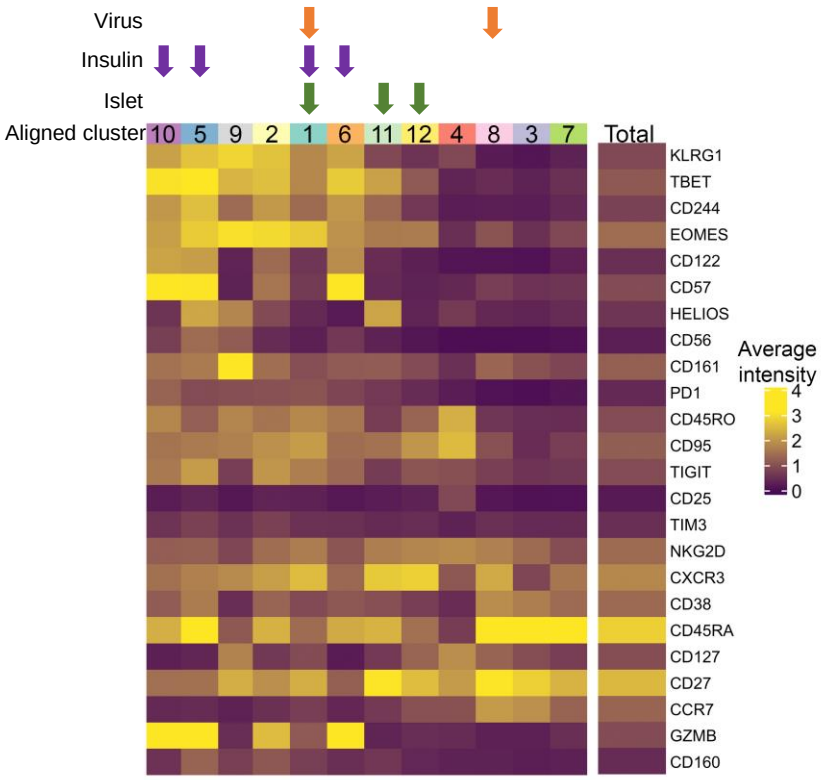

Supplemental Figure 5. Twelve CD8⁺ T cell phenotypes of T1D subjects. A heatmap of mean absolute arcsinh-transformed expression of 24 markers for the twelve aligned clusters determined in Figure 1 and total CD8⁺ T cells from all T1D subjects (n=46). Arrows indicate clusters which were consistently dominant among cells of a particular antigen specificity (orange, virus; purple, insulin; green, islet).

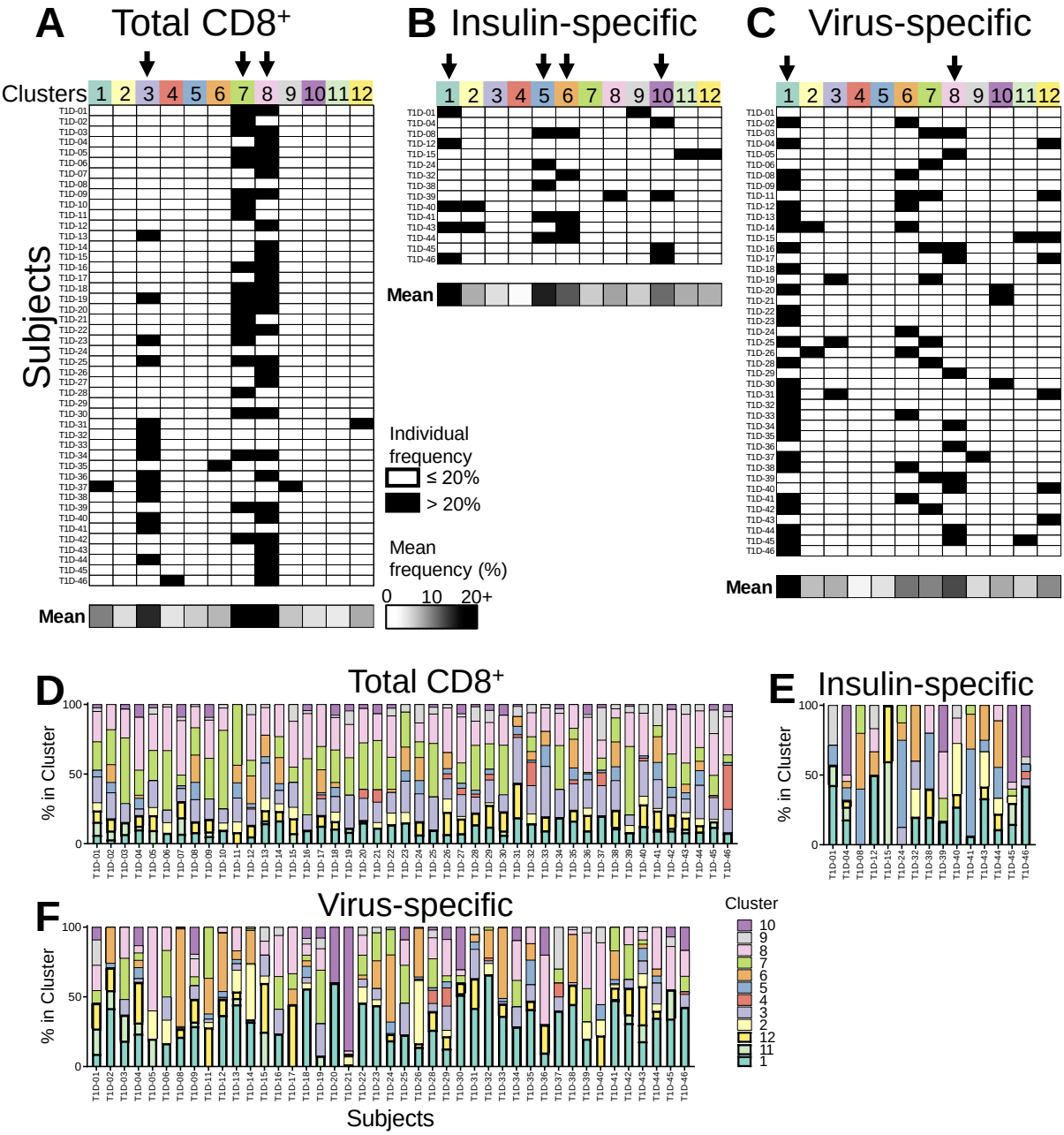

Supplemental Figure 6. Antigen-specific CD8⁺ T cells from T1D subjects comprise multiple distinct phenotypes. The DISCOV-R analysis method was applied to total CD8⁺ and antigen-specific T cells from T1D subjects (n=46) assayed with our Tmr-CyTOF panel. Twelve aligned clusters common across all samples were defined by hierarchical metaclustering. **(A-C)** Clusters comprising more than 20% of cells for an individual are indicated in black for **(A)** total CD8+ T cells (n=46), and subjects with at least 5 Tmr⁺ cells among **(B)** insulin-specific cells (n=15) and **(C)** virus-specific cells (n=43). Arrows indicate clusters predominant in at least 25% of samples; the detached bottom row indicates the mean frequency of cells within a cluster for all individuals on a scale from 0% (white) to 20%+ (black). **(D-F)** The percent of each of the twelve clusters were assessed for **(D)** total CD8+ T cells (n=46), and subjects with at least 5 Tmr⁺ cells among **(E)** insulin-specific cells (n=15) and **(F)** virus-specific cells (n=43). The 3 clusters that are most dominant among islet-specific cells across subjects (clusters 1, 11, and 12) have heavy outline and are stacked at the bottom. Tmr, tetramer.

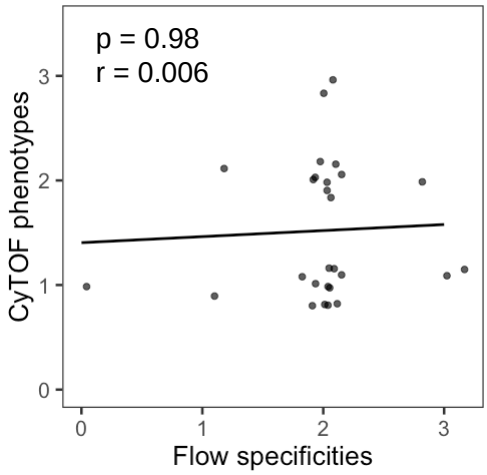

Supplemental Figure 7. The number of predominant phenotypes of islet-specific CD8⁺ T cells does not correlate with the number of positive islet antigen specificities. A subset of the T1D subjects (n = 27) that were analyzed by the DISCOV-R method were also assayed by flow cytometry for frequency of CD8⁺ T cells specific for individual epitopes (PPI, GAD, and IGRP) separately. The number predominantly occupied clusters (phenotypes comprising >20% of islet-specific cells) determined by DISCOV-R plotted against the number of positive (>0.02%) islet antigen specificities determined by flow cytometry. Jitter was added to visualize stacked points. Statistical significance was determined by Spearman correlation.

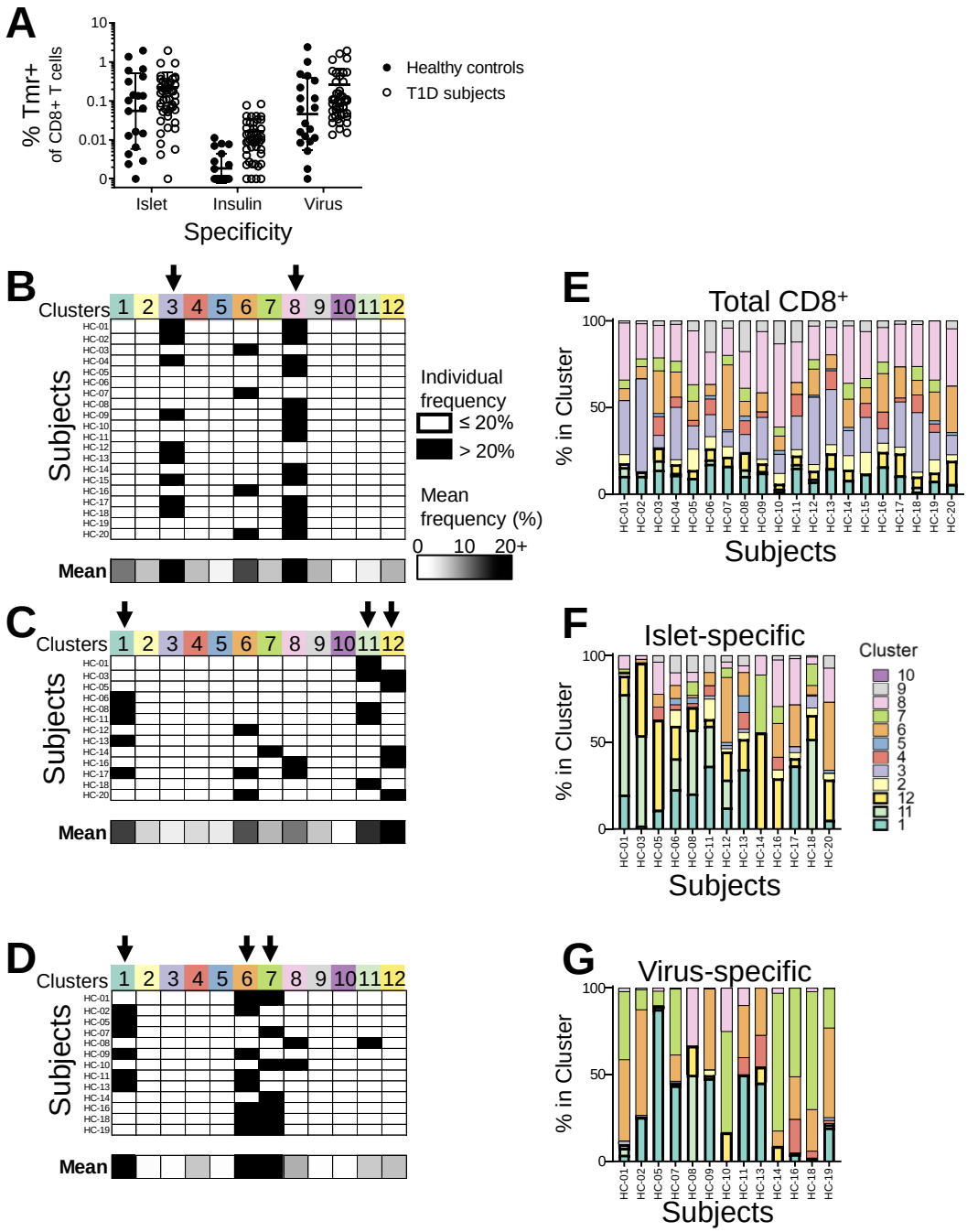

Supplemental Figure 8. Antigen-specific CD8⁺ T cell frequency and islet-specific cell phenotype do not differ between healthy controls and T1D subjects. Healthy controls (n=20) were assayed with our Tmr-CyTOF panel and included in the DISCOV-R analysis as in Figure 1. **(A)** Frequencies of antigen-specific (Tmr⁺) within total CD8⁺ T cells among healthy controls (n=20) and T1D subjects (n=46) was compared using a two-way ANOVA with Sidak test for multiple comparisons. **(B-D)** Clusters comprising more than 20% of cells for an individual are indicated in black for **(B)** total CD8+ T cells (n=20), and individuals with at least 5 Tmr⁺ cells among **(C)** islet-specific cells (n=13) and **(D)** virus-specific cells (n=13). Arrows indicate clusters predominant in at least 25% of samples; the detached bottom row indicates the mean frequency of cells within a cluster for all individuals on a scale from 0% (white) to 20%+ (black). **(E-G)** The percent of each of the twelve clusters were assessed for **(E)** total CD8+ T cells (n=20), and subjects with at least 5 Tmr⁺ cells among **(F)** insulin-specific cells (n=13) and **(G)** virus-specific cells (n=13). The 3 clusters that are most dominant among islet-specific cells across subjects (clusters 1, 11, and 12) have heavy outline and are stacked at the bottom. Tmr, tetramer.

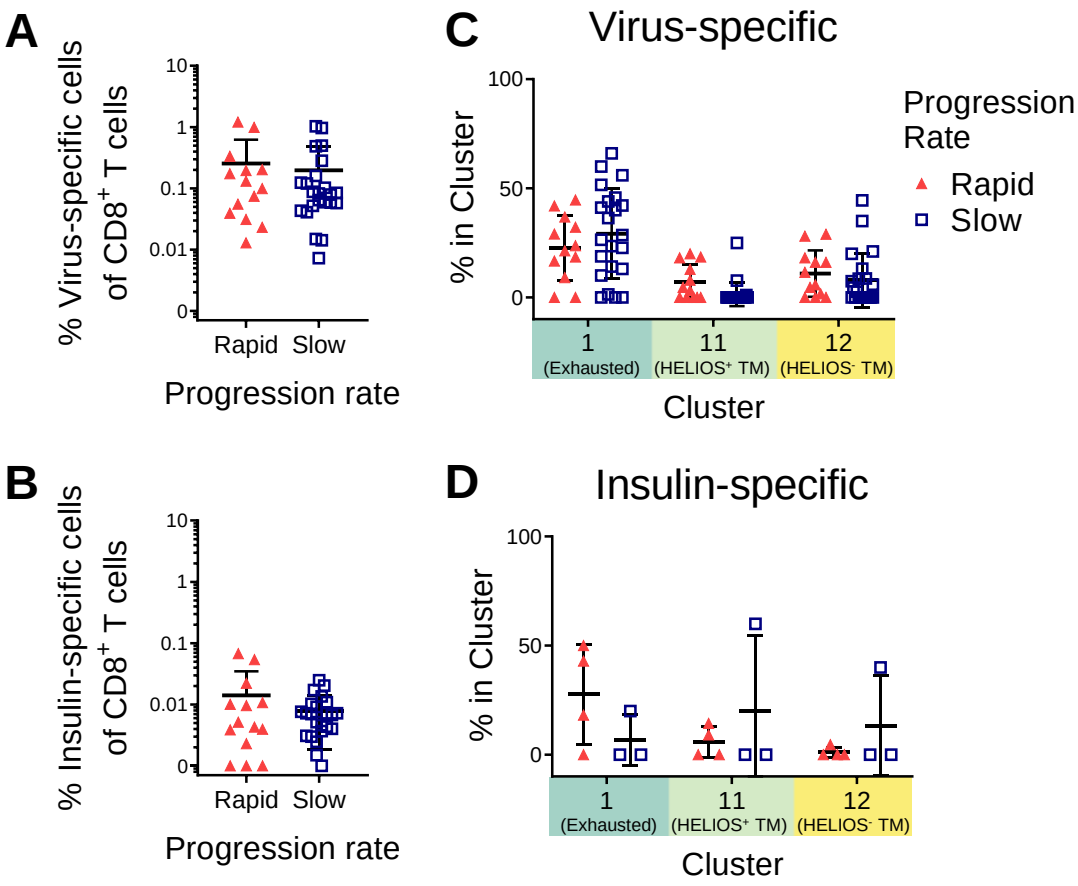

Supplemental Figure 9. Virus- and insulin-specific CD8⁺ T cell frequencies and phenotypes do not differ by rate of disease progression. Frequency of **(A)** virus- or **(B)** insulin-specific cells among CD8⁺ T cells was assessed for rapid (n=14) and slow (n=23) T1D progressors using a Mann-Whitney test. Frequency the three common islet-specific clusters was assessed for rapid and slow T1D progressors with five or more Tmr⁺ events using a two-way ANOVA with Sidak test for multiple comparisons among **(C)** virus- (n=12 rapid, n=22 slow) or **(D)** insulin-specific (n= 4 rapid, n=3 slow) CD8⁺ T cells. Black horizontal lines with error bars represent mean ± SD. Tmr, tetramer; TM, transitional memory.

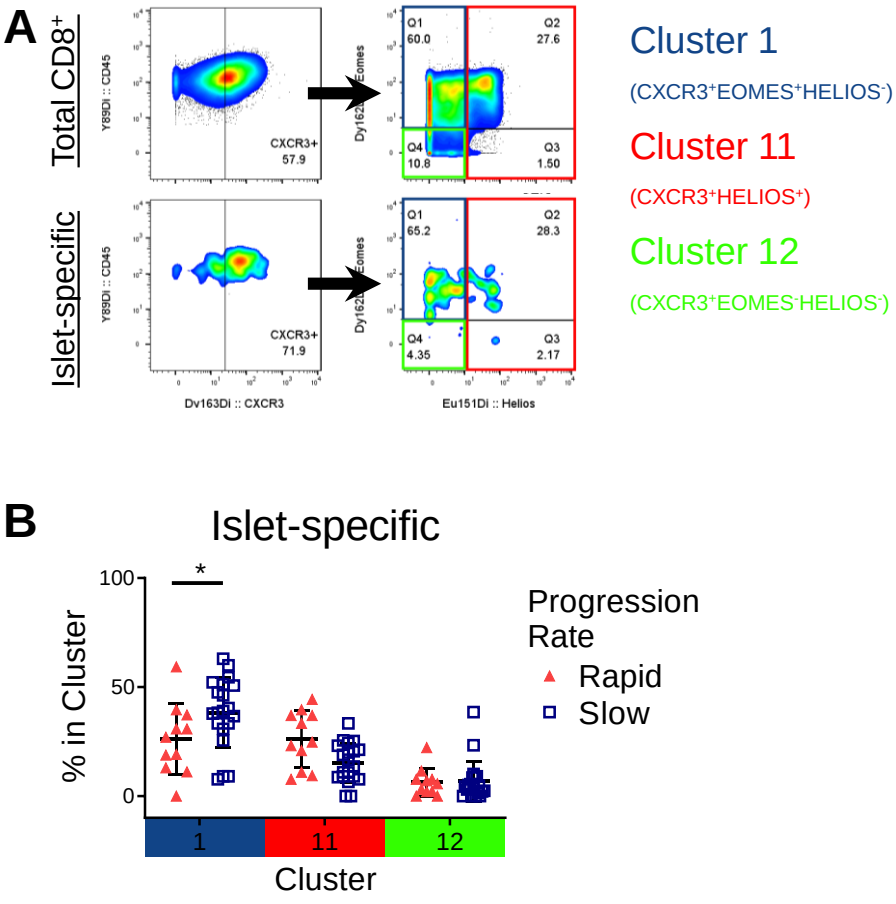

Supplemental Figure 10. Frequency of manually-gated islet-specific phenotypes is associated with rate of disease progression. T1D samples were manually gated for a small number of selected markers that distinguished clusters 1 ($CXCR3^+HELIOS^-EOMES^+$), 11 ($CXCR3^+HELIOS^+$), and 12 ($CXCR3^+HELIOS^-EOMES^-$). **(A)** Representative gating strategy for one individual (T1D-41). **(B)** Frequency of islet-specific $CD8^+$ T cells among the three manually gated populations for rapid (n=11) and slow (n=20) T1D progressors with 5 or more Tmr^+ events. Statistical comparisons were made using a two-way ANOVA with Sidak test for multiple comparisons. Black horizontal lines with error bars represent mean ± SD. Tmr, tetramer; *, $p<0.05$.

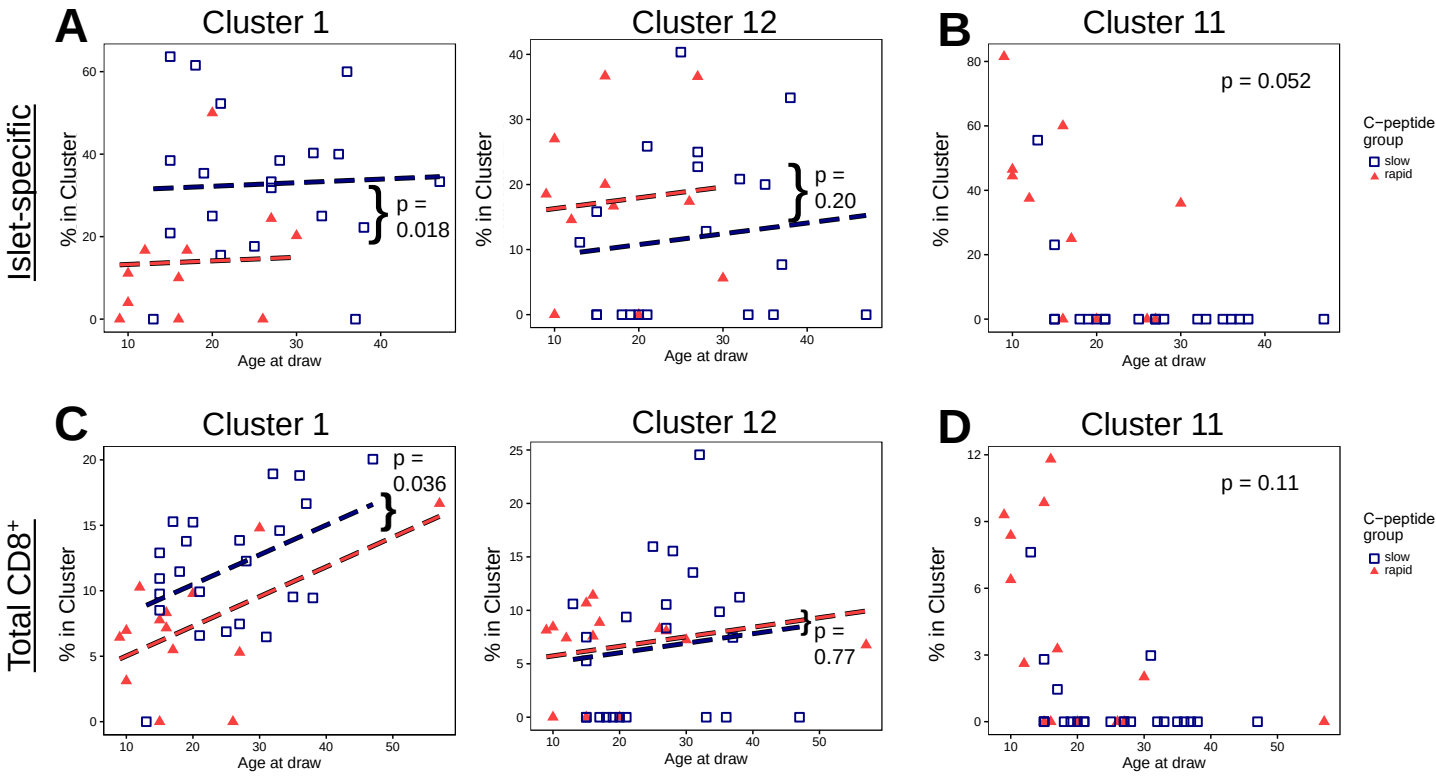

Supplemental Figure 11. Differential phenotypes of islet-specific and total CD8⁺ T cells in rapid and slow progressors remain after accounting for age. Lines show best-fit models for rapid and slow progression groups, using a common slope for **(A & B)** islet-specific and **(C & D)** total CD8⁺ T cells. Significance values shown are for differences between groups in a **(A & C)** linear or **(B & D)** logistic model with age at draw as a covariate. Interaction terms for age x group were not significant for all but islet-specific cells in cluster 11 and were not included in any of the final models.

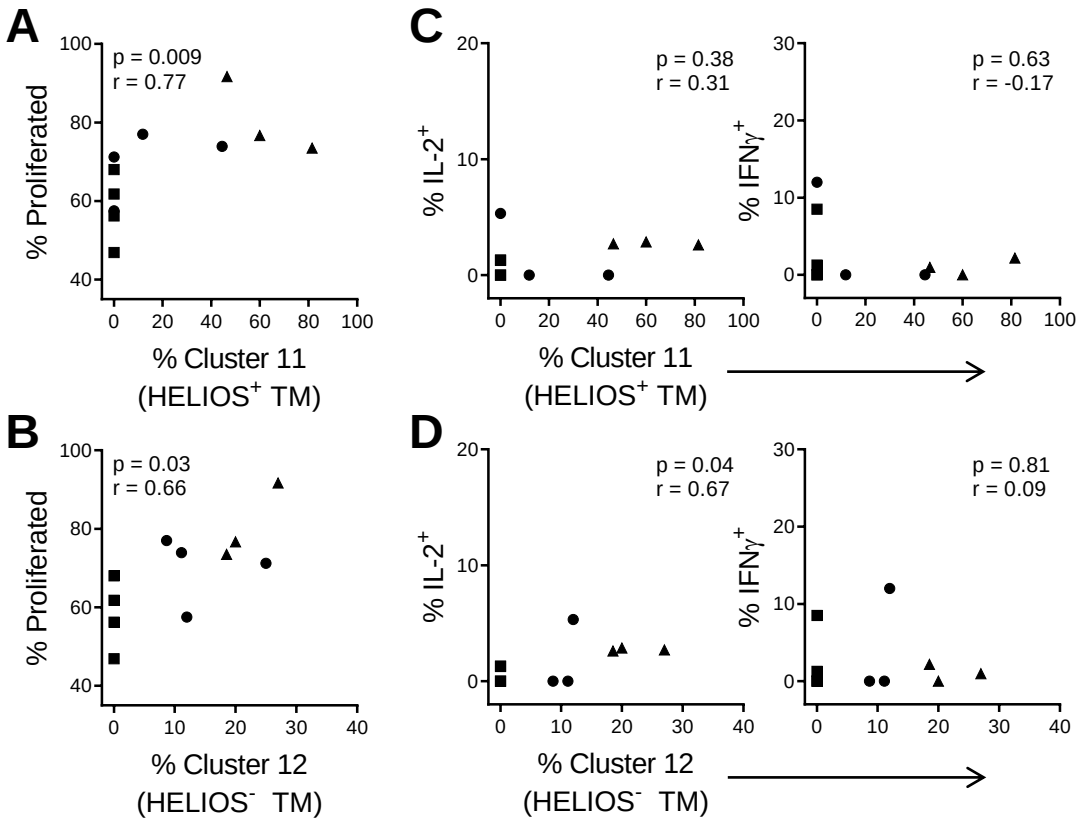

Supplemental Figure 12. Islet-specific CD8⁺ T cells with abundant cluster 11 or 12 phenotype are hyperproliferative but produce limited levels of cytokines, IL-2 and IFN-γ. PBMC from T1D subjects (n=11) with varying frequencies of cluster 11 or 12 among their islet-specific cells were stimulated with anti-CD3 plus anti-CD28. Cells were assayed by flow cytometry to identify islet-specific (Tmr⁺) CD8⁺ T cells (Supplemental Figure 13). Frequency of proliferated cells among islet Tmr⁺ cells after 5 days of stimulation, plotted against frequency of **(A)** cluster 11 or **(B)** cluster 12 determined by mass cytometry for each individual (n=11). Frequency of IL-2 and IFN-γ positive cells among islet Tmr⁺ cells after 6 hours of stimulation, plotted against frequency of **(C)** cluster 11 or **(D)** cluster 12 determined by mass cytometry for each individual (n=10); no substantial cytokine production (<1%) was observed in the absence of stimulation. Statistical significance was determined by Spearman correlation. Tmr, tetramer; TM, transitional memory.

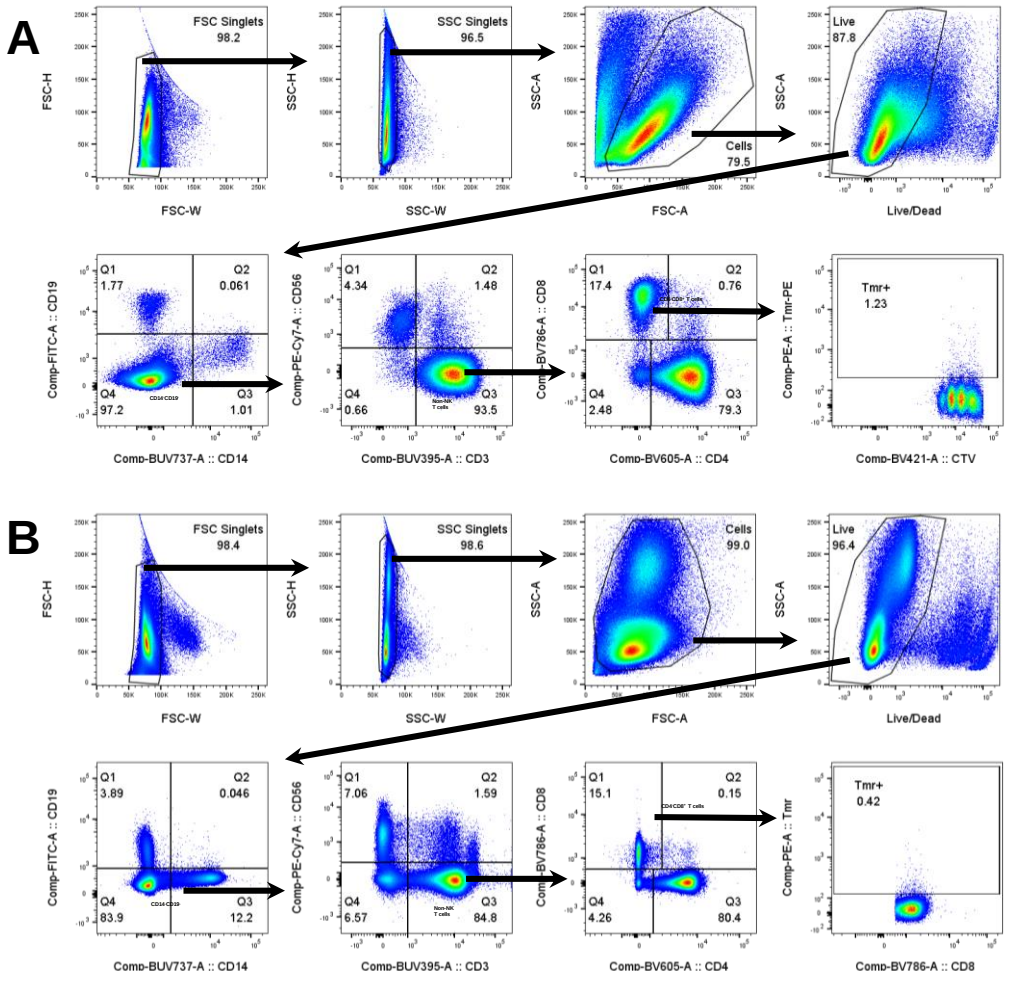

Supplemental Figure 13. Gating strategy to identify islet-specific CD8⁺ T cells using flow cytometry panels. Cells from one representative individual (T1D-34) after stimulation with anti-CD3 plus anti-CD28 were gated for singlet live $CD14^-CD19^-CD56^-CD3^+CD4^-CD8^+$ ($CD8^+$ T cells) that were positive for pooled islet Tmr using the **(A)** proliferation panel or **(B)** cytokine panel. Tmr^+ gating was guided by HLA-A2 negative and PPI-specific $CD8^+$ T cell clone-spiked control samples. The same gates were applied to stimulated and unstimulated samples from the same subject. Tmr, tetramer; CTV, cell trace violet.

Supplemental Table 1. Antigen-specific CD8$^+$ T cell mass cytometry phenotyping panel.

Mass	Target	Clone	Supplier	Cocktail
89	CD45	HI30	Fluidigm	Surface
141	CD45RO	UCHL1	Biolegend*	Surface
142	CD57	HCD57	Fluidigm	Surface
143	CD45RA	HI100	Fluidigm	Surface
144	CD38	HIT2	Fluidigm	Surface
145	CD8	RPA-T8	Biolegend*	Surface
146	CD4	RPA-T4	Biolegend*	Surface
147	KLRG1	14C2A07	Biolegend*	Surface
148	CD14	RMO52	Fluidigm	Surface
149	CD127	A019D5	Fluidigm	Surface
151	Helios	22F6	Biolegend*	Intracellular
152	CD160	BY55	Biolegend*	Surface
153	Tim3	F382E2	Fluidigm	Surface
154	CD3	UCHT1	Fluidigm	Surface
155	TIGIT	MBSA43	eBioscience*	Surface
156	CD25	M-A251	Biolegend*	Surface
158	CD27	L128	Fluidigm	Surface
159	CD161	HP3G10	Fluidigm	Surface
160	Tbet	4B10	Fluidigm	Intracellular
162	Eomes	WD1928	eBioscience*	Intracellular
163	CXCR3	G025H7	Fluidigm	Surface
164	CD95	DX2	Fluidigm	Surface
165	CD19	HIB19	Fluidigm	Surface
166	NKG2D	ON72	Fluidigm	Surface
167	CCR7	G043H7	Fluidigm	Surface
168	Tmr	--	--	Tetramer
169	Tmr	--	--	Tetramer
170	CD122	Tu27	Fluidigm	Surface
171	Granzyme B	GB11	Fluidigm	Intracellular
173	2B4	C1.7	Biolegend*	Surface
174	Tmr	--	--	Tetramer
175	PD1	EH12.2H7	Fluidigm	Surface
176	CD56	NCAM16.2	Fluidigm	Surface
191/193	Iridium (cell size)	--	Fluidigm	Iridium
194-198	Cisplatin (viability)	--	Enzo Life Sciences	Cisplatin

*Unlabeled purified antibodies were conjugated to metal isotopes using Maxpar X8 Antibody Labeling Kits (Fluidigm) as per manufacturer's instructions.

Supplemental Table 2. HLA-A*0201 tetramers.

Specificity Pool	Origin	Position/ Protein	Peptide Sequence	Metal Isotope Labels		
				Er168	Er169	Yb174
Islet	PPI	15-24	ALWGPEPAAA	X		X
	GAD65	114-123	VMNILLQYVV	X		X
	IGRP	265-273	VLFGLGFAI	X		X
	pplAPP	5-13	KLQFLIVL	X		X
Insulin	Insulin	B 10-18	HLVEALYLV		X	X
Virus	CMV	pp65	NLVPMVATV	X	X	
	EBV	LMP2	CLGGLLTMV	X	X	

Abbreviations: PPI, preproinsulin; GAD, glutamic acid decarboxylase; IGRP, islet-specific glucose-6-phosphatase catalytic subunit-related protein; pplAPP, prepro-islet amyloid polypeptide; CMV, cytomegalovirus; EBV, Epstein-Barr virus.

Supplemental Table 3. Individual subject demographics.

Cohort		ID	Gender	Race	Age (years) at draw	Age (years) at diagnosis	Disease duration (years) at draw
Healthy controls		HC-01	Male	White	5	NA	NA
		HC-02	Female	White	13	NA	NA
		HC-03	Male	White	14	NA	NA
		HC-04	Female	White	16	NA	NA
		HC-05	Male	White	17	NA	NA
		HC-06	Female	Multiracial	18	NA	NA
		HC-07	Male	Unknown	18	NA	NA
		HC-08	Female	White	19	NA	NA
		HC-09	Male	White/Asian	20	NA	NA
		HC-10	Female	White	20	NA	NA
		HC-11	Female	Multiracial	20	NA	NA
		HC-12	Female	Asian	20	NA	NA
		HC-13	Female	White	20	NA	NA
		HC-14	Male	White	20	NA	NA
		HC-15	Female	White	24	NA	NA
		HC-16	Male	Black	25	NA	NA
		HC-17	Female	White	31	NA	NA
		HC-18	Male	Unknown	37	NA	NA
		HC-19	Male	White	41	NA	NA
		HC-20	Male	Asian	43	NA	NA
T1D disease progression rate[a]	Rapid Progression	T1D-01[e]	Male	Unknown	9	7.2	1.9
		T1D-02[e]	Female	Unknown	10	10.0	0.9
		T1D-03	Female	White	10	9.0	1.8
		T1D-04[d]	Male	White	12	7.7	4.8
		T1D-05	Female	Unknown	15	10.8	4.2
		T1D-06	Male	White	15	13.5	1.9
		T1D-07[e]	Male	White	16	12.5	3.5
		T1D-08[d]	Male	White	16	13.7	3.2
		T1D-09	Female	White	17	16.8	0.8
		T1D-10	Female	White	20	17.2	3.8
		T1D-11	Female	Unknown	26	21.5	4.7
		T1D-12	Female	White	27	26.8	1.1
		T1D-13	Female	White	30	28.7	2.3
		T1D-14	Male	Asian	57	54.9	2.5
	Slow Progression	T1D-15	Male	White	13	4.9	8.9
		T1D-16[e]	Female	White	15	4.6	10.7
		T1D-17	Female	White	15	8.5	7.3
		T1D-18	Male	White	15	9.3	6.6
		T1D-19	Female	White	15	10.5	5.4
		T1D-20	Female	White	17	10.8	6.3
		T1D-21[e]	Female	Unknown	18	13.0	5.7
		T1D-22[d]	Female	White	19	14.5	5.2
		T1D-23	Female	White	20	13.5	6.8
		T1D-24	Female	White	21	15.7	5.6
		T1D-25[e]	Male	White	21	14.0	7.1
		T1D-26	Female	White/Nat Amer	25	21.0	5.0
		T1D-27	Male	Unknown	27	17.5	10.3
		T1D-28	Male	White	27	20.4	6.9
		T1D-29	Female	White	28	22.1	5.9
		T1D-30	Female	White	31	26.0	5.6
		T1D-31[d]	Female	White	32	27.2	5.5
		T1D-32[c]	Female	White	33	5.4	28.2
		T1D-33	Male	White	35	29.7	6.1
		T1D-34[e]	Female	White	36	24.6	12.2
		T1D-35	Male	White	37	26.4	11.0
		T1D-36[c]	Female	White	38	24.8	13.4
		T1D-37	Female	White	47	17.3	30.7
T1D disease duration[b]	<5 years	T1D-38	Female	White	12	11.4	1.6
		T1D-39[c]	Female	White	15	13.9	1.7
		T1D-40[e]	Female	White	25	22.4	2.9
		T1D-41[e]	Male	White	37	35.2	1.8
	≥5 years	T1D-42[e]	Male	White	18	7.7	10.4
		T1D-43	Female	White	25	18.9	6.4
		T1D-44[e]	Female	White/Nat Amer	35	16.3	19.4
		T1D-45[c]	Male	White	46	36.9	10.1
		T1D-46[c]	Female	White	61	11.9	49.2

[a] Rapid progressors are less than 5 years from diagnosis and have undetectable C-peptide (<0.05 ng/mL); slow progressors are 5 or more years from diagnosis but retain detectable C-peptide (>0.1 ng/mL).

[b] < 5 years from diagnosis and have detectable C-peptide (>0.1 ng/mL); ≥ 5 years from diagnosis and have undetectable C-peptide (<0.05 ng/mL).

[c] Sample was used in reproducibility testing.

[d] A second sample from a later time point was also assayed.

[e] Sample was tested in functional studies.

Nat Amer, Native American.